Colossal magnetoresistance and relaxation phenomena

1998 J. Phys.: Condens. Matter 10 9769

(http://iopscience.iop.org/0953-8984/10/43/021)

J. Phys.: Condens. Matter **10** (1998) 9769–9782. Printed in the UK PII: S0953-8984(98)93558-5

Colossal magnetoresistance and relaxation phenomena

L M Fisher†, A V Kalinov†, S E Savel'ev†, I F Voloshin† and A M Balbashov‡

† All-Russian Electrical Engineering Institute, 12 Krasnokazarmennaya Street, 111250 Moscow, Russia

‡ Moscow Power Engineering Institute, 14 Krasnokazarmennaya Street, 105835 Moscow, Russia

Received 20 April 1998, in final form 13 July 1998

Abstract. The magnetization and magnetoresistance of $La_{1-x}A_xMnO_3$ (A = Sr, Ca) single crystals have been studied in the static regime. The same characteristics have been investigated as functions of time in response to a sharp change of the magnetic field. The magnetic moment M, dynamic magnetic susceptibility χ', and resistivity ρ are found to relax noticeably in the samples with A = Sr ($x = 0.3, 0.35$). These parameters are shown to relax approximately logarithmically over time. The relaxation is temperature dependent, and diminishes when the temperature is far from that of the magnetic transition. The resistivity and magnetization do not relax when the field direction is reversed instantaneously. The static and relaxation properties observed are interpreted in the framework of a simple phenomenological model.

1. Introduction

The phenomenon of colossal negative magnetoresistance (CMR) in the manganese-based perovskite-like compounds $La_{1-x}A_xMnO_3$ [1], and analogous compounds, has recently drawn close attention. In spite of the numerous thorough investigations, the origin of the phenomenon is still under discussion. There are a variety of facts concerning the CMR phenomenon which is found in the vicinity of the magnetic transition accompanied by a transition of metal–insulator (semiconductor) type [2–11]. Some models involving double-exchange interaction, scattering on the magnetic polarons, metal–insulator transition etc are commonly used to discuss the possible nature of the CMR phenomenon. The role of the phase-separated ferromagnetic–antiferromagnetic states in such systems is emphasized in the review [4]. Nevertheless, the physical nature of the phases in this system is under question. The dependence of the resistivity on the magnetic field in the perovskite-like materials has been studied in numerous papers [1, 2, 4, 8, 10–14]. In particular, a detailed study of the dependence of the resistivity ρ on the magnetic field H and magnetization M has been performed for the system $La_{1-x}Sr_xMnO_3$ in [2]. The authors of that paper showed experimentally that the dependences of ρ on the temperature T, magnetic field H, and concentration x for $T > T_c$ may be described by the simple equation

$$-\frac{\rho(H)-\rho(0)}{\rho(0)} = C(x)\left(\frac{M(H)}{M_s}\right)^2 \tag{1}$$

where $M_s \approx 4\mu_B$ (per Mn site) is the saturation magnetization and $C(x)$ is the coefficient which changes from about 4 to 1 in the x-range 0.1–0.4 and does not depend on H and T. This scaling of ρ with M fails for $T < T_c$: at low H the resistivity keeps approximately to a constant value, whereas the magnetization M increases with the magnetic field.

0953-8984/98/439769+14$19.50

Additional information about the physical properties of the CMR systems can be obtained by means of measurements of the relaxation phenomena in these media. Relaxation of the magnetization, after a sharp change of the external magnetic field, was observed in many magnetics. Sometimes the relaxation continues for many seconds, and is described by a logarithmic law (see, for example, the investigation of the relaxation process in thin ferromagnetic films in [15]). For systems with CMR, the observation of the magnetic relaxation can assist one in tracking the correlation between ρ and M in the process of the relaxation, because during this process the magnetization changes with time, whereas the external magnetic field H remains constant. Therefore, the main focus of this paper is on a study of the relaxation effects in a system with CMR. We have performed the investigation of these mixed systems for the most interesting region—in the vicinity of the magnetic transition, where the negative magnetoresistance is very pronounced.

$La_{1-x}A_xMnO_3$ single crystals with A = Sr, Ca were investigated in our study. The static behaviour of the magnetization and resistivity is in agreement with known results (see [2]). The noticeable relaxation of the magnetization, dynamic susceptibility, and resistivity has been observed for samples with A = Sr ($x = 0.3, 0.35$). These relaxations are shown to be most pronounced at the transition temperature, and to be approximately logarithmic functions of time. The main features observed may be qualitatively explained within the framework of a simple approach based on the consideration of a three-well potential with a spatially distributed activation energy.

2. Experiment

All of the samples studied were bulk single crystals of $La_{1-x}A_xMnO_3$ prepared by the floating-zone melting procedure with radiation heating (see, for example, [16]). One crystal with A = Ca ($x = 0.22$) and others with A = Sr ($x = 0.1, 0.2, 0.3, 0.35$) were studied. The as-grown crystals were distorted cylinders about 10 mm in length and 3–5 mm in diameter. The samples of $La_{0.7}Sr_{0.3}MnO_3$ and $La_{0.88}Ca_{0.22}MnO_3$ were examined carefully by x-ray diffraction (Siemens D-500) and using an electron beam microanalyser (CAMEBAX SX-50). Both crystals revealed diffraction patterns that were sufficiently nearly perfect, and homogeneous phase compositions.

We measured the static magnetic moment (magnetization M) of the as-grown crystals or their fragments using a vibrating-sample magnetometer (VSM) in the magnetic field (up to 1.5 T) of an electromagnet with a core diameter of 160 mm. Its magnetic field settling time was several seconds. The dynamic magnetic (ac) susceptibility $\chi = \chi' + i\chi''$ measured by the conventional inductive method at frequencies in the range 10^2–10^3 Hz and the electrical resistivity ρ were studied in the magnetic field of the electromagnet mentioned above or that of a smaller electromagnet made from an audio-frequency gap choke. The latter electromagnet, with a special current supply, generated a stable magnetic field up to 3 kOe with a settling time of several milliseconds.

The ac susceptibility and resistivity measurements were carried out on plate-like samples cut from the crystals. The current leads and potential probes were connected to the samples with indium. Such connections gave a low-impedance electrical contact that permitted us to use transport current values of up to 100 mA without any thermal problems. The pick-up coil used for the ac susceptibility measurements was wound around the sample in its middle region between the potential contacts. The copper–constantan thermocouple was in direct thermal contact either with the sample or with the highly thermally conducting dielectric plate holding the sample. These elements were put into a box made of thin silicon plates, with outer dimensions of about $12 \times 12 \times 60$ mm^3. The copper wire coil and manganin

double-wire heater were wound around this box. This thermal container was wrapped in Teflon tape and put into the ducting under a cooling gas flow. The thermal container used in the VSM measurements was almost the same. The holding and sweeping of the temperature were maintained by an IGC-4 temperature controller (Oxford Instruments). This system permitted us to hold the temperature of the sample within 0.1 K and to measure it with an absolute accuracy better than 1 K.

In our experiment we studied the magnetic field, temperature, and temporal dependences of the magnetization M and resistivity ρ at different mutual orientations of the magnetic field and current relative to the crystallographic directions. We did not see any remarkable orientation effects.

We would like to draw attention to some features of the characteristics studied near the magnetic transition temperature T_c which are revealed most noticeably for $La_{1-x}Sr_xMnO_3$ at $x = 0.3$ and $x = 0.35$. Interest in these compounds is high, as they are extremely popular candidates for applications. Furthermore, all of the results presented in the plots will be for the sample with $x = 0.3$ only. The sample with $x = 0.35$ exhibits almost the same features, except a slightly different value of T_c.

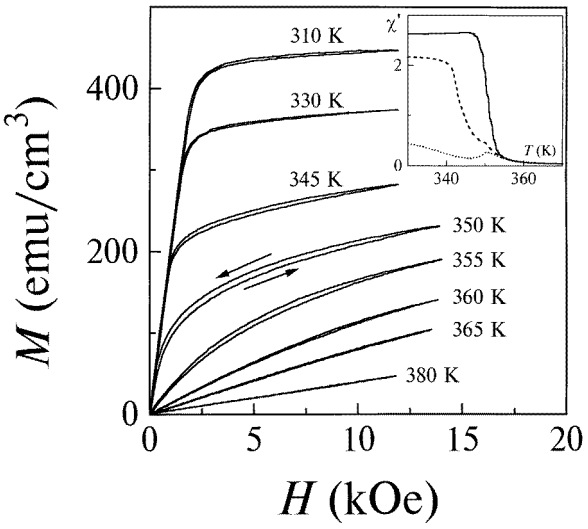

Figure 1. The magnetization curves obtained at various temperatures in the vicinity of the magnetic transition temperature. The arrows show the directions of the magnetic field change. In the inset, the dynamic magnetic susceptibility χ' is shown as a function of the temperature for the different magnetic fields: $H = 0$: solid curve; $H = 500$ Oe: dashed curve; and $H = 1$ kOe: dotted curve. The two fields are parallel to each other.

2.1. Experimental results

At the beginning of our study, we made measurements of the static magnetic and electrical characteristics of our samples. The main results are presented in figures 1 and 2. According to the measurements of the temperature dependences of the resistivity and magnetic susceptibility at the ac-field amplitude of 10 Oe, their sharp changes are observed at the same temperature (see the insets to figures 1 and 2). The critical temperature T_c may be evaluated as $T_c \approx 352$ K.

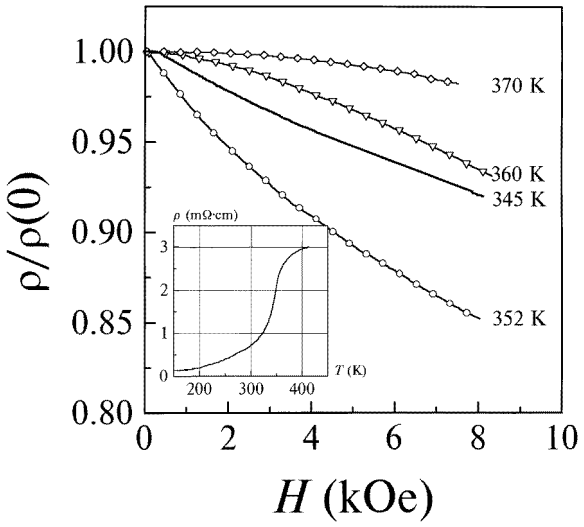

Figure 2. The magnetic field dependence of the normalized resistivity $\rho(H)/\rho(H=0)$ at the temperatures given in the plot. The inset shows the resistivity versus the temperature at the magnetic field $H = 0$.

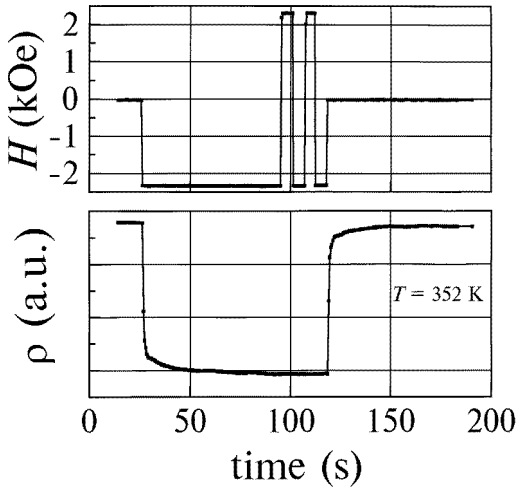

Figure 3. The changes of the resistivity, in arbitrary units (lower panel), in response to step-like changes of the magnetic field (upper panel). Note that sharp $H \leftrightarrow -H$ steps cause no changes in and thus no relaxation of ρ.

Consider the magnetization curves for several temperatures near T_c that are shown in figure 1. At 380 K the magnetization changes linearly with the external magnetic field, as in paramagnetic materials. As the temperature decreases, a bend of the $M(H)$ curve appears and then displaces to lower fields. Also, the slope of $M(H)$ near $H = 0$ increases sharply, and saturates at $T \approx T_c$. Such a behaviour of $M(H)$ is demonstrated also by the solid curve representing $\chi'(T)$ in the inset to figure 1. As a result, all of the magnetization curves have conjoint linear portions near $H = 0$ at $T < T_c$. Note that the nonlinear parts

of the magnetization curves prove to be sufficiently dependent on the field sweeping rate as to be manifested in a hysteresis-like behaviour (the magnetization curves in figure 1 were recorded at a sweeping rate of about 1 kOe min^{-1}). This effect is most pronounced in the vicinity of the transition temperature T_c. The hysteresis of the magnetization was observed to decrease with the decrease of the sweeping rate.

The variation of the electrical resistivity with the external magnetic field in the vicinity of T_c depends noticeably on the field sweeping rate too. To get almost static experimental curves $\rho(H)$, we used a low enough field sweeping rate, of about 0.1 kOe min^{-1}. The results of the measurements are presented in figure 2 for several temperatures near T_c. The main features of the dependences $\rho(H, T)/\rho(0, T)$ near T_c that we would like to outline are the following:

(i) at temperatures higher than T_c the resistivity depends weakly on H, and the shape of the $\rho(H)$ curve is convex;

(ii) at temperatures very close to T_c the magnetic field dependence of the resistivity is more pronounced, and, contrary to the case for $T > T_c$, the curve $\rho(H)$ is concave;

(iii) at temperatures lower than T_c the magnetic field change of the resistance is lower than for the case where $T \approx T_c$; the curves are concave too.

As was mentioned above, the results of the $M(H)$ and $\rho(H)$ measurements were rather sensitive to the magnetic field sweeping rate. Therefore, we studied the response of our sample to step changes of the magnetic field from some value H_1 to another value H_2. A qualitative illustration of such responses of $\rho(H, t)$ is presented in figure 3. The experiment was done using the 'fast' magnet described above. In the upper panel of the figure, the sequence of the magnetic field changes is shown. The curve in the lower panel is the reaction of the magnetoresistance of the sample. The resistivity is clearly seen to change—

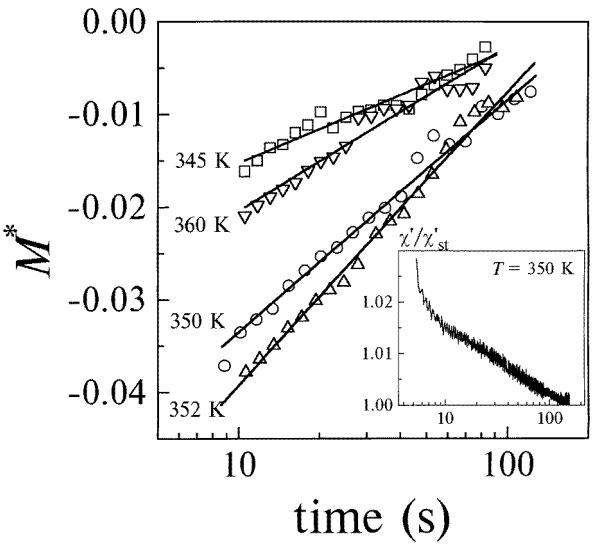

Figure 4. The relaxation of the normalized magnetization in response to a sharp change of the magnetic field ($0 \rightarrow 9$ kOe) at the temperatures in the vicinity of the magnetic transition temperature. The solid lines show the best fit to a logarithmic law. In the inset, the relative relaxation of the magnetic susceptibility χ' in the magnetic field $H = 1$ kOe (from $H = 0$) is shown.

at first quickly after the sharp drop of H from zero to -3 kOe, and then a slow relaxation process is observed. The timescale of the relaxation process goes up to dozens of seconds. A similar relaxation of ρ is observed after a change of H from -3 kOe to zero.

It is interesting to note that the relaxation occurs only for the steps in which the magnetic field H is changed in modulus. If a fast step between H and $-H$ occurs, no relaxation process in $\rho(H)$ is observed. This fact is illustrated in figure 3 by the absence of a resistivity change after H is stepped from -3 kOe to 3 kOe.

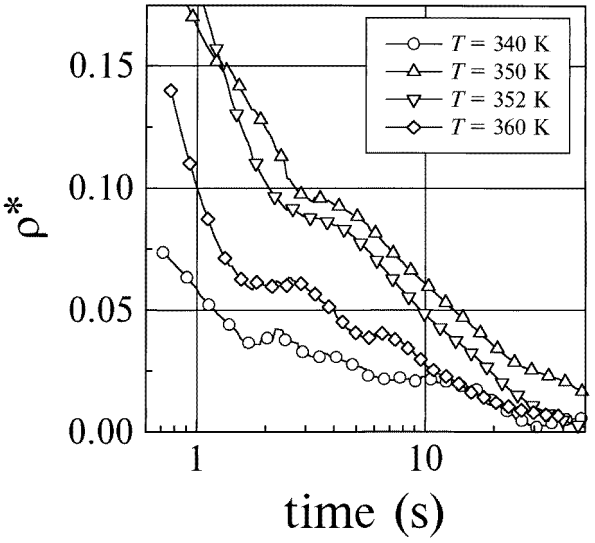

Figure 5. The time dependence (relaxation) of the normalized resistivity in response to a sharp change of the magnetic field ($0 \rightarrow 3$ kOe) at the temperatures specified in the plot.

We studied the relaxation phenomenon over a wide temperature range. The relaxation processes were observed to occur both in the resistivity and in the magnetization in the vicinity of T_c. Some of the results of our measurements are presented in figures 4 and 5. The resistivities and magnetizations in these figures are normalized with respect to the jumps of these values as follows:

$$\rho^*(t) = [\rho(t) - \rho(H_2)]/|\rho(H_1) - \rho(H_2)|$$

and

$$M^*(t) = [M(t) - M(H_2)]/|M(H_1) - M(H_2)|$$

where $\rho(H_1)$, $\rho(H_2)$, $M(H_1)$, and $M(H_2)$ are the static values of these characteristics. The resistivity and magnetization relaxations become close to a logarithmic law within a few seconds after a magnetic field jump for all of the temperatures studied. Unfortunately, measurements of the relaxation process of the magnetization were available only for the magnetic field of the large electromagnet, having a time response of several seconds. For this reason, we had to omit the data close to the origin of the time axis. It should be emphasized that relaxation in the resistivity was always accompanied by relaxation in the magnetization and vice versa. The strongest relaxation process is observed near the critical temperature T_c, but it becomes weaker at higher and lower temperatures. (The relaxation of the magnetic susceptibility χ' is shown in the inset to figure 4.)

An interesting difference between the relaxations of ρ and M was observed. The relaxation of the resistivity in response to the magnetic field change from H_1 to H_2 follows a logarithmic law for any values $|H_1| \neq |H_2|$. For example, the changes of H from 0 to

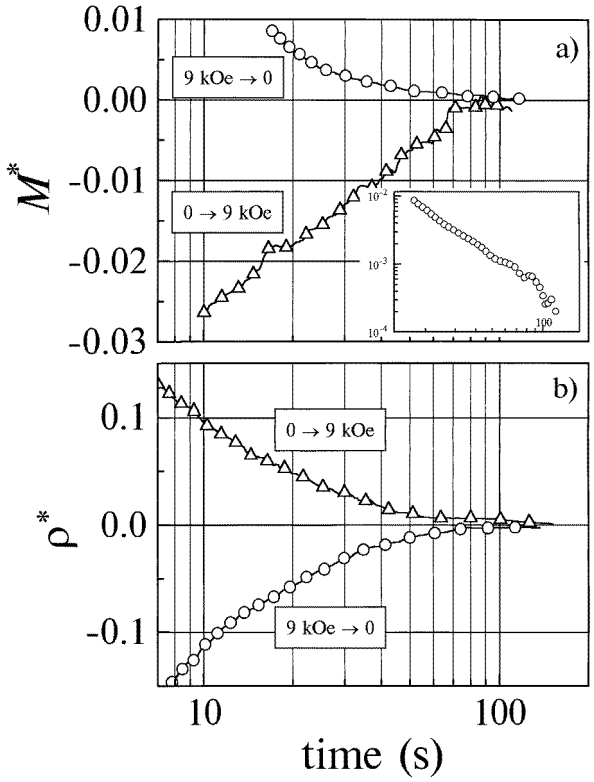

Figure 6. The relaxation of the normalized magnetization (a) and normalized resistivity (b) in response to sharp changes of the magnetic field ($0 \leftrightarrow 9$ kOe) at $T = 350$ K. These dependences are shown to be logarithm-like except in the case of the magnetization relaxation in response to the 9 kOe $\leftrightarrow$ 0 jump; that relaxes according to a power law (see the inset in the upper panel).

9 kOe and from 9 kOe to 0 (see the lower panel in figure 6) evoke logarithm-like changes of $\rho^*(t)$ in the interval $10 < t < 100$ s which are approximately symmetrical with respect to the line $\rho^* = 0$. In contrast to that of the resistivity, the logarithm-like relaxation of the magnetization was observed for $H_2 \neq 0$ only. In the case where $H_2 = 0$, the relaxation process changes radically and is described by a power function. This result is presented in the upper panel of figure 6 and its inset. The relaxation of the susceptibility has the same asymmetry as the magnetization.

We also have looked for a relaxation effect in the samples with the other stoichiometry (A = Ca, $x = 0.22$ and A = Sr, $x = 0.1, 0.2$). For some samples a small relaxation effect has been observed in response to the $H_2 = 0$ magnetic field change; however, our experimental resolution limits us to estimating the relaxation magnitude as being at least one order of magnitude lower than that presented above. So, we cannot reach any definite conclusions about relaxation in these samples.

3. Discussion

Let us analyse our experimental data and compare them with some known results. To deduce features of the CMR, it is useful to plot the dependence of the resistivity versus

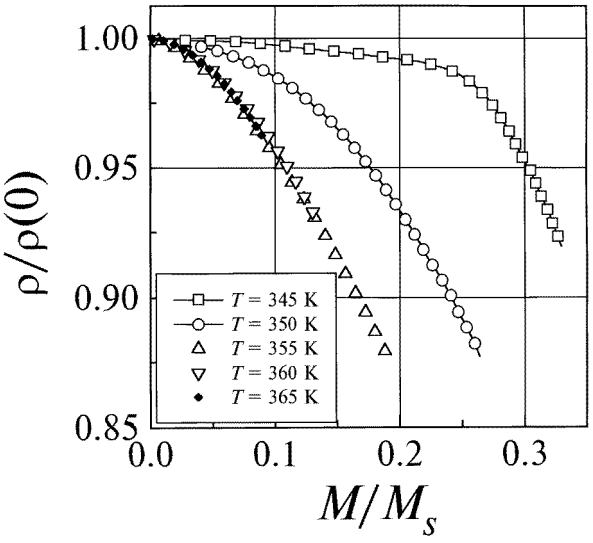

Figure 7. The scaling of the dimensionless resistivity with the dimensionless magnetization (in units of the saturated magnetization). This scaling is shown to fail at temperatures just below the transition temperature.

the magnetization. Figure 7 shows the change of the reduced resistivity $\rho(H)/\rho(0)$ with the magnetization M/M_s. The dependences $\rho(H)/\rho(0) = F(M/M_s)$ in figure 7 are obtained by merging our experimental data for $M(H)$ and $\rho(H)$ (see figures 1 and 2). For $T > T_c$ these dependences are clearly seen to be described by the universal function $\rho(H)/\rho(0) = A(M/M_s)^{1.6}$, which is close to equation (1). This scaling law fails below the temperature T_c. That is, reduction of the temperature by just 2 K from T_c leads to a significant deviation of the experimental dependence from the scaling law. In particular, at temperatures $T < T_c$ an appreciable negative magnetoresistance emerges only after a considerable change in the magnetization M. This inhibition of the negative magnetoresistance is observed in the low-magnetic-field region, where the linear part of the magnetization curve (figure 1) is realized. At higher fields where $M(H)$ has saturation-like behaviour, the negative magnetoresistivity is very pronounced. Such a behaviour of $\rho(M)/\rho(0)$ was discussed previously in [2]. So, since the static characteristics studied coincide with known ones (see, for example, [2, 11]), we believe our samples to be typical.

The observed static and relaxation characteristics of our samples are not unique, and can be met in other (not perovskite) magnetic systems. A quite similar behaviour of the magnetoresistance was observed, for example, for some antiferromagnetic compounds upon suppression of the AFM state by a high magnetic field [17]. These features of the magneto-resistance appear to be common for some magnetic materials, and are related to some peculiarities of the system behaviour near the magnetic transition where different magnetic phases may coexist [4]. Relaxation processes occur in some magnetic media also. The logarithm-like relaxation in some magnetics is known to be an attribute of an ensemble of small FM particles (see, for example, [15]). For such ensembles the relaxation has been interpreted in terms of thermally assisted remagnetization of the particles, taking into account a dispersion of the energy barriers which separate the states with different directions of magnetization. Therefore, these circumstances provide grounds for considering that the static and relaxation properties observed should not depend critically on a certain mechanism

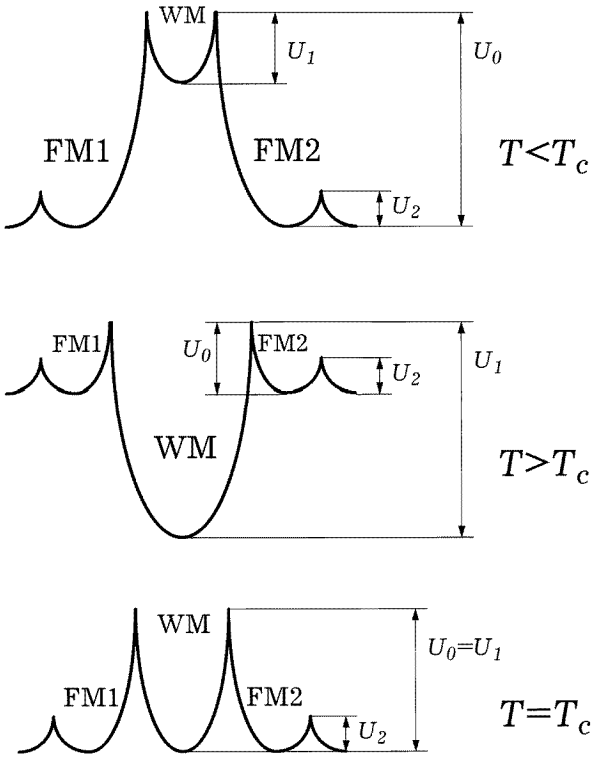

Figure 8. The qualitative picture of the phase coexistence for temperatures near the magnetic transition.

of the magnetoresistivity. So, we hope that these properties may be described within the framework of some phenomenological approach.

3.1. Possible interpretation

To construct a simple phenomenological model, we consider the following. Let two separate magnetic phases with different electric properties coexist in perovskite materials [4]. For example, these phases may differ in the charge carrier density, but it is assumed that there are no crystal imperfections. The concentrations of these phases can change under the action of the magnetic field H owing to a thermally activated transformation of one phase into the other.

Let us accept that in the vicinity of the magnetic transition T_c this system is divided into a ferromagnetic (FM) phase with a low resistivity and some antiferromagnetic or paramagnetic phase with a high resistivity and weak magnetization (the WM phase). In our consideration, we do not use any specific features of this phase, so it does not matter which type of highly resistive phase with weak magnetization we consider. Moreover, neither our experiment nor theory give any information about the type of magnetic ordering of this phase. The WM phase dominates at $T > T_c$, whereas the FM phase gives a more noticeable contribution at $T < T_c$. Also, let the FM phase be divided into phases with oppositely directed magnetizations (FM1 and FM2). The phases are separated from each other by energy barriers. (In figure 8, the energy states of the phase coexistence are shown

schematically.) Consequently, the probabilities of the transitions between these states during the characteristic time τ_0 are proportional to the multipliers $\exp(-U_0/T)$, $\exp(-U_1/T)$, and $\exp(-U_2/T)$ for the following transitions: FM $\rightarrow$ WM state, WM $\rightarrow$ FM state, and FM1 $\rightarrow$ FM2 state, respectively. The phase concentrations $c_{\uparrow\uparrow}$ (FM along the $\boldsymbol{H}$-direction), $c_{\uparrow\downarrow}$ (WM), and $c_{\downarrow\downarrow}$ (FM opposite to the $\boldsymbol{H}$-direction) are defined by the following equations:

$$\begin{aligned}
&c_{\uparrow\uparrow} + c_{\uparrow\downarrow} + c_{\downarrow\downarrow} = 1 \\
&\frac{\partial c_{\uparrow\uparrow}}{\partial \tau} = -c_{\uparrow\uparrow}\exp(-(U_0 + M_0H)/T) - c_{\uparrow\uparrow}\exp(-(U_2 + M_0H)/T) \\
&\qquad\qquad + c_{\uparrow\downarrow}\exp(-U_1/T) + c_{\downarrow\downarrow}\exp(-(U_2 - M_0H)/T) \\
&\frac{\partial c_{\downarrow\downarrow}}{\partial \tau} = -c_{\downarrow\downarrow}\exp(-(U_0 - M_0H)/T) - c_{\downarrow\downarrow}\exp(-(U_2 - M_0H)/T) \\
&\qquad\qquad + c_{\uparrow\downarrow}\exp(-U_1/T) + c_{\uparrow\uparrow}\exp(-(U_2 + M_0H)/T)
\end{aligned} \tag{2}$$

where M_0 is the FM phase magnetization, and $\tau = t/\tau_0$ is dimensionless time. It is assumed here that the energy barriers for the transitions FM $\rightarrow$ WM and FM1 $\leftrightarrow$ FM2 change by the value M_0H under exposure to a magnetic field. To obtain equations describing the static and relaxation electromagnetic properties of our multiphase medium, we should write out the relations of the magnetic moment and resistivity using the FM and WM concentrations. We assume that these relations may be written as follows:

$$\begin{aligned}
&\rho(H) = (c_{\uparrow\uparrow}(H) + c_{\downarrow\downarrow}(H))\rho_1 + c_{\uparrow\downarrow}(H)\rho_2 \\
&M(H) = M_0(c_{\uparrow\uparrow}(H) - c_{\downarrow\downarrow}(H))
\end{aligned} \tag{3}$$

where ρ_1 and ρ_2 are field-independent specific resistivities of the FM and WM phases, respectively ($\rho_1 < \rho_2$). Of course, these equations are phenomenological, and we cannot pretend that they give an absolutely correct description of the $\rho(H)$ and $M(H)$ behaviour. Nevertheless, they become exact in the limit case if the phases are connected in series, and give a good approximation for a small change of the FM phase concentration with H in the case of a complex parallel–series connection.

Using these equations and the set (2), it is possible to obtain a set of temporal equations which allow us to analyse both the static and the relaxation properties of the resistivity and magnetization of our system:

$$\begin{aligned}
&\frac{\partial m}{\partial \tau} = \beta\left[r\sinh\left(\frac{M_0H}{T}\right) - m\cosh\left(\frac{M_0H}{T}\right)\right] \qquad m = M/M_0 \\
&\frac{\partial r}{\partial \tau} = \gamma\left[-r\cosh\left(\frac{M_0H}{T}\right) + m\sinh\left(\frac{M_0H}{T}\right) + \alpha(1-r)\right] \qquad r = \frac{\rho_2 - \rho}{\rho_2 - \rho_1}
\end{aligned} \tag{4}$$

where

$$\begin{aligned}
&\beta = \exp(-U_0/T) + 2\exp(-U_2/T) \\
&\gamma = \exp(-U_0/T) \\
&\alpha = 2\exp(-(U_1 - U_0)/T).
\end{aligned}$$

Let us, first, analyse the static properties. To do this, we substitute $\partial r/\partial t = \partial m/\partial t = 0$ into the set (4), and obtain the static magnetic field dependence of r and m as follows:

$$\begin{aligned}
&r(H) = \frac{\alpha}{\alpha + [\cosh(M_0H/T)]^{-1}} \\
&m(H) = r(H)\tanh(M_0H/T) = \frac{\alpha\tanh(M_0H/T)}{\alpha + [\cosh(M_0H/T)]^{-1}}.
\end{aligned} \tag{5}$$

To compare the results obtained using our model with the experiment, we need to discuss how the parameters change near the transition temperature T_c. At first, we assume that the energy spectrum changes very sharply at the transition from the situation which is presented in figure 8 for $T > T_c$ to the situation shown in figure 8 for $T < T_c$. So, we shall use below the feature that the barriers change substantially, from $U_0 \gg U_1$ at $T < T_c$ to $U_0 \ll U_1$ at $T > T_c$. In principle, both M_0 and $\rho_{1,2}$ can also change with temperature. Moreover, M_0 equals zero at the temperature $T_{c1} > T_c$ at which the ferromagnetic state begins to form. Nevertheless, for simplicity we assume that the critical temperatures T_{c1} and T_c are essentially different, so we do not have to consider the temperature dependences of M_0, ρ_1, and ρ_2 near T_c. Also, taking into account smooth temperature dependences of M_0, ρ_1, and ρ_2 would not qualitatively change the results obtained.

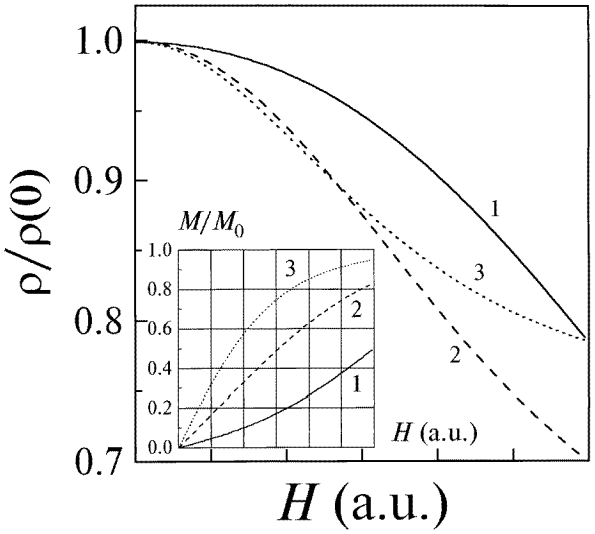

Figure 9. The calculated dependences of the dimensionless resistivity versus magnetic field for different values of the α-parameter: line 1: $\alpha = 0.1$; line 2: $\alpha = 0.5$; and line 3: $\alpha = 2$. In the inset, the calculated $M(H)$ dependences for the same α-values are shown.

Furthermore, we take into account the facts that the barrier height U_0 increases with decreasing temperature near T_c and that the FM phase concentration begins to grow sharply. This leads to a noticeable change of the parameter α from $\alpha = 2\exp(-U_1/T) \ll 1$ for $T > T_c$ to a value of about or above unity for $T \leqslant T_c$. According to equations (5) and (3), the resistivity drops in the vicinity of T_c at $H = 0$, which coincides with a dielectric–metal transition. Figure 9 shows the magnetic field dependences of M and ρ at temperatures lower and higher than T_c calculated by means of equations (5) and (3). To compare the calculated dependences with the experimental results, we use three different values of the parameter α. The inset in figure 9 demonstrates the calculated behaviour of the magnetization $M(H)/M_0$ for $T > T_c$ (curve 1), $T \approx T_c$ (curve 2), and $T < T_c$ (curve 3). The results of the calculations agree qualitatively with the experiment (figure 1), at least at high magnetic fields. The main discrepancy is observed at low fields. The calculated curves differ from each other at different temperatures $T < T_c$, whereas the experimental curves $M(H)/M_0$ almost coincide at low H. The $\rho(H)$ curve for $T > T_c$ (curve 1) is shown to be proportional to H^2, which is close to the experimental result (figure 2). The maximum of the calculated magnetoresistance is obtained at $T \approx T_c$ (curve 2). Below

T_c the magnetoresistance decreases (curve 3). It is clearly seen that these curves correlate qualitatively with the experimental results.

To study the behaviour of ρ at low magnetic fields, we calculated the dependence of the resistivity on the magnetization. Figure 10 shows the dependences of $\rho/\rho(H = 0)$ on M/M_0 calculated for different temperatures. Curves 1, 2, and 3 correspond to $T > T_c$ ($\alpha \ll 1$), $T \approx T_c$ ($\alpha \approx 1$), and $T < T_c$ ($\alpha > 1$), respectively. The trend in the changes of the curves calculated for the model agrees qualitatively with our experiment. Indeed, the $\rho(M)$ dependence becomes slower at low M with the temperature decrease. These results agree also with the data of [2] (compare the inset to figure 10 and the data from [2]). Some discrepancy between the experiment and our calculation is seen in the form of the $\rho(M)$ curves. The calculated curves demonstrate a monotonic decrease of $\rho(M)$, whereas the experimental curves exhibit a resistivity that is practically independent of the magnetization for low M for $T < T_c$.

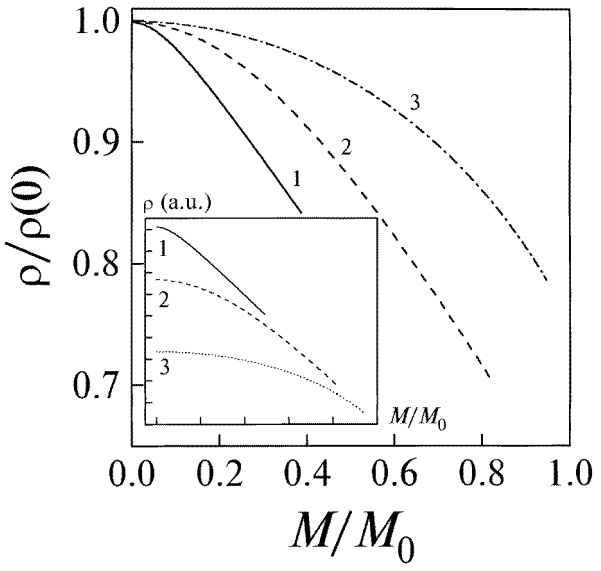

Figure 10. The calculated dependences of the dimensionless resistivity versus magnetization for different values of the α-parameter: line 1: $\alpha = 0.1$; line 2: $\alpha = 0.5$; and line 3: $\alpha = 2$. In the inset, the calculated $\rho(M)$ dependences for the same α-values are shown.

The discrepancies between our experiment and theory as regards the behaviour of the magnetization and resistivity at low magnetic fields can be eliminated by making a single additional assumption. We can assume that the energy barrier between the FM and WM phases changes more slowly with H at low H and for $T < T_c$ than we had assumed in our calculations ($U_0(H) = U_0(0) \pm M_0 H$). Unfortunately, we do not know of a physical explanation for such a behaviour of $U_0(H)$.

Let us analyse now the temporal dependence of the characteristics studied in response to the fast magnetic field change from H_1 to H_2. In accordance with our approach, after the field jump the change of the magnetic phase concentrations occurs. This is not an instantaneous process, because of the presence of the barriers. Using equation set (4), one can obtain the temporal dependences of the magnetization and resistivity:

$$\delta r(\tau) = \Delta r \exp(-\lambda_1 \tau)$$
$$\delta m = \Delta r \tanh\left(\frac{M_0 H_2}{T}\right) \exp(-\lambda_1 \tau) + \left[\Delta m - \Delta r \tanh\left(\frac{M_0 H_2}{T}\right)\right] \exp(-\lambda_2 \tau) \qquad (6)$$

where

$$\Delta m = m_{st}(H_1) - m_{st}(H_2) \qquad \Delta r = r_{st}(H_1) - r_{st}(H_2)$$
$$\lambda_1 = \gamma\left[\alpha + (\cosh(M_0H_2/T))^{-1}\right]$$
$$\lambda_2 = \beta\cosh\left(\frac{M_0H_2}{T}\right) + \gamma\cosh\left(\frac{M_0H_2}{T}\right) - \frac{\gamma}{\cosh(M_0H_2/T)} \qquad \lambda_1 \ll \lambda_2 \tag{7}$$

where m_{st} and r_{st} are the static solutions defined by (5). Here it was assumed that the barrier between the two FM phases was the smallest one, i.e., that the speed of the FM phase remagnetization is high ($\beta \gg \gamma$, $\beta \gg \gamma\alpha$). Therefore, two relaxation times appear. The shorter time relates to the FM phase remagnetization, whereas the other time is that of the transition between the FM and WM phases.

This set of equations allows us to understand the absence of the relaxation in response to $H \leftrightarrow -H$ steps in our experiment. For such jumps the difference of the static resistivities $\Delta r = 0$, because r is an even function of H (see (5)). As a result, only the fast temporal term (for the FM1 $\leftrightarrow$ FM2 transition) is retained in equation (6).

Equations (6) allow us to explain the asymmetric magnetization relaxation for the jumps of H from $H_1 \neq 0$ to $H_2 = 0$ and back from $H_1 = 0$ to $H_2 \neq 0$. According to equation (6), the relaxation of the magnetization for the jump of H to zero ($H_2 = 0$) is accomplished in a short time $1/\lambda_2$, whereas for the jump of H from zero to $H_2 \neq 0$ this relaxation is accomplished in a long time $1/\lambda_1$. It is interesting that the relaxation of the resistivity is accomplished in the long time $1/\lambda_1$ in both cases.

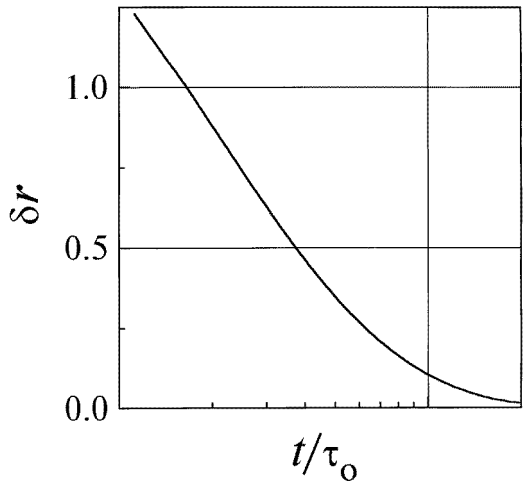

Figure 11. The resistivity relaxation calculated from equation (8).

It should be noted that, according to equation (6), M and ρ prove to be exponential functions of time. The logarithm-like relaxations, which were experimentally observed, can be connected with the dispersion of the barrier heights [15]. Averaging expression (6) and keeping the temporal term involving the long time, we obtain

$$\delta r(\tau) = \Delta r \int \mathrm{d}U_0 \; f(U_0)\exp(-\exp(-U_0/T)[\alpha + (\cosh(M_0H/T))^{-1}]\tau) \tag{8}$$

where $f(U_0)$ is the distribution function for the barrier height. If this function is rather wide and smooth, one will obtain the logarithm-like relaxation. The results of this calculation are

presented in figure 11. The relaxation is seen to be described by a logarithm-like law, which converts to an exponential law at long times. These results agree well with the experimental relaxation of ρ.

4. Conclusions

The static and relaxation properties of the magnetization and resistivity of single crystals of the perovskite system $La_{1-x}Sr_xMnO_3$ with x up to 0.35 have been studied in detail. Appreciable relaxations have been observed in compounds with $x = 0.3$ and 0.35. We found the relaxation process to be most pronounced in the close vicinity of the magnetic transition temperature T_c. Relaxations of the magnetization and resistivity accompany each other always. The relaxation process is described by a logarithmic law for most cases, except the case for switching off the external magnetic field, when the relaxation of the resistivity remains logarithm-like whereas the magnetization relaxes according to a power law. The other striking feature of this material is the absence of relaxation for a jump of the external field from H to $-H$. Both the relaxation and the static properties studied may be qualitatively explained within the proposed simple phenomenological model of a phase-separated ferromagnetic–antiferromagnetic state with different resistivities of the FM and WM phases.

Acknowledgments

The authors would like to thank Dr K I Kugel and Dr S G Karabashev for stimulating discussions and helpful remarks. This work was supported by the Russian Basic Research Foundation, project No 96-02-17889.

References

[1] Jin S, Tiefel T H, McCormack M, Fastnacht R A, Ramesh R and Chen L H 1994 *Science* **264** 413
[2] Urushibara A, Moritomo Y, Arima T, Asamitsu A, Kido G and Tokura Y 1995 *Phys. Rev.* B **51** 14 103
[3] Knizek K, Jirak Z, Pollert E, Zounova F and Vratislav S 1992 *J. Solid State Chem.* **100** 292
[4] Nagaev E L 1996 *Sov. Phys.–Usp.* **39** 781
[5] Schiffer P, Ramirez A P, Bao W and Cheong S W 1995 *Phys. Rev. Lett.* **75** 3336
[6] Ju H L, Gopalakrishnan J, Peng J L, Li Q, Xiong G C, Venkatesan T and Greene R L 1995 *Phys. Rev.* B **51** 6143
[7] Kimura T, Tomioka Y, Kawahara H, Asamitsu A, Tamura M and Tokura Y 1996 *Science* **274** 1698
[8] Ramirez A P 1997 *J. Phys.: Condens. Matter* **9** 8171
[9] von Helmolt R, Wecker J, Samwer K, Haupt L and Barner K 1994 *J. Appl. Phys.* **76** 6925
[10] Chahara K-i, Ohno T, Kasai M and Kozono Y 1993 *Appl. Phys. Lett.* **63** 1990
[11] Fontcuberta J, Martínez B, Seffar A, Piñol S, García-Muñoz J L and Obradors X 1996 *Phys. Rev. Lett.* **76** 1122
[12] von Helmolt R, Wecker J, Holzapfel B, Schultz L and Samwer K 1993 *Phys. Rev. Lett.* **71** 2331
[13] Mahendiran R and Raychaudhuri A K 1996 *Phys. Rev.* B **54** 16 044
[14] Hwang H Y, Cheong S-W, Ong N P and Batlogg B 1996 *Phys. Rev. Lett.* **77** 2041
[15] Iglesias O, Badia F, Labarta A and Balcells Ll 1995 *J. Magn. Magn. Mater.* **140–144** 399
[16] Balbashov A M, Karabashev S G, Mukovskiy Ya M and Zverkov S A 1996 *J. Cryst. Growth* **167** 365
[17] Kunkel H P, Zhou X Z, Stampe P A, Cowen J A and Williams G 1996 *Phys. Rev.* B **54** 16 039